HHS Public Access

Author manuscript

Hum Pathol. Author manuscript; available in PMC 2023 January 01.

Published in final edited form as:

Hum Pathol. 2022 January ; 119: 15–27. doi:10.1016/j.humpath.2021.09.009.

Morphological heterogeneity in beta-catenine-mutated hepatocellular carcinomas:implications for tumor molecular classification☆

Michael Torbenson, M.D.[a,*], **Chantal E. McCabe, Ph.D.**[d], **Daniel R. O'Brien, Ph.D**[d], **Jun Yin, Ph.D.**[e], **Tiffany Bainter, M. PH**[e], **Nguyen H. Tran, M.D.**[b], **Saba Yasir, MBBS**[a], **Zongming Eric Chen, M.D., Ph.D.**[a], **Renu Dhanasekaran, M.D.**[f], **Keun Soo Ahn, M.D.**[g], **Lewis R. Roberts, M.B.**[c], **Chen Wang, Ph.D.**[d]

[a]Mayo Clinic Department of Pathology and Laboratory Medicine, United States

[b]Department of Oncology, Mayo Clinic, Rochester, MN, United States

[c]Division of Gastroenterology and Hepatology, Mayo Clinic, Rochester, MN, United States

[d]Department of Health Sciences Research, Mayo Clinic, Rochester, MN, United States

[e]Division of Clinical Trials and Biostatistics, Mayo Clinic, Rochester, MN, United States

[f]Division of Gastroenterology and Hepatology, Stanford University, Stanford, CA, United States

[g]Department of Surgery, Keimyung University School of Medicine, Keimyung University Dongsan Hospital, Daegu, Republic of Korea

Summary

Beta-catenin (*CTNNB1*) is commonly mutated in hepatocellular carcinoma (HCC). *CTNNB1*-mutated HCC has important clinical correlates, such as being immune cold and less likely to respond to immune checkpoint inhibitor therapies. It remains unclear, however, if they are a morphologically homogenous group of tumors. To better understand the association between the morphology, *CTNNB1* mutations, and other molecular features, a detailed study of 338 The Cancer Genome Atlas cases was performed. A characteristic histological morphology was strongly associated with *CTNNB1* mutations but was present in only 58% of *CTNNB1*-mutated HCCs. Tumors with *APC* mutations tended to have the classic morphology; those with *AXIN* mutations did not. Pseudoglands are a key feature of the classic morphology, and they were associated with *CTNNB1* mutations, male gender, specific *CTNNB1* mutation site, and lack of *TP53* mutations. Differential gene expression analysis stratified by the presence/absence of pseudoglands identified 60 differentially expressed genes (FDR <5%); clustering according to

☆Competing interests: None.

*Corresponding author. Department of Pathology and Laboratory Medicine, Mayo Clinic, 200 First Street, SW, Rochester, MN 55905, USA. Torbenson.Michael@mayo.edu (M. Torbenson).

Authors' contributions

M.T., S.Y., Z.E.C., D.R.O., C.E.M., and C.W. designed the study. M.T., S.Y., and Z.E.C. contributed to histology review. M.T., R.D., K.S.A., L.R.R., and C.W. collected the data. M.T., D.R.O., C.E.M., C.W., J.Y., Z.E.C., and T.B. analyzed the data. M.T., N.H.T., D.R.O., C.E.M., C.W., and J.Y. drafted the article. All authors edited the article.

Appendix A. Supplementary data

Supplementary data to this article can be found online at https://doi.org/10.1016/j.humpath.2021.09.009.

these differentially expressed genes revealed three groups of tumors, one with pseudoglands and a strong association with genes regulated by Wnt signaling; within this group, *TP53* mutations were associated with a loss of the typical morphology of *CTNNB1*-mutated HCCs. When stratified by gender, further differential gene expression showed Wnt-regulated genes were associated with pseudoglands in men but not women. These findings indicate HCC with *CTNNB1* mutations are morphologically heterogeneous, with gene penetrance for morphology dependent in part on gender, specific *CTNNB1* mutations, and co-occurring *TP53* mutations. This heterogeneity has important implications for the classification of HCC.

Keywords

CTNNB1; APC; AXIN; Survival; Differential gene expression

1. Introduction

Hepatocellular carcinomas (HCCs) have heterogeneous molecular aberrations [1]. Beta-catenin (*CTNNB1*) mutations are among the most common mutations in HCC, present in up to 35% of cases [2]. Beta-catenin is a key protein of the Wnt signaling pathway, with activating mutations leading to enhanced signaling of the Wnt pathway. Additional key proteins are encoded by *AXIN* and *APC*; these proteins normally suppress Wnt pathway activation, and inactivating mutations can lead to increased Wnt pathway signaling. HCCs with *CTNNB1* mutations are more likely to be well-differentiated, have a thin trabecular growth pattern (synonym is microtrabecular), have pseudoglands (synonym is microacini), and produce bile [3–5], histological findings that together create a composite morphological pattern for *CTNNB1*-mutated HCCs. Recent studies have identified important clinical correlates for *CTNNB1*-mutated tumors, with a subset that has less inflammation by gene expression analysis (“immune cold”) [6] and a subset that appears less likely to respond to checkpoint inhibitor therapies [7]. Clinical outcome studies have been inconsistent, with studies showing less aggressive [4] and more aggressive behavior [2] for *CTNNB1*-mutated HCCs.

An important question for morphological/molecular tumor classification is whether *CTNNB1*-mutated HCCs represent a homogenous entity. For example, the reported correlations between *CTNNB1* mutations and the classic morphology are statistically strong, but a significant proportion of HCCs with *CTNNB1* mutations lack the classic morphology [3–5]. On the other hand, anecdotal experience has shown that HCCs can sometimes have the classic morphology but lack *CTNNB1* mutations. To better understand the morphology of *CTNNB1*-mutated HCCs and to refine the morphological-molecular classification, detailed studies were undertaken of the clinical-histological-molecular correlations for *CTNNB1*-mutated HCCs.

2. Materials and methods

2.1. Case selection

The study was approved by the Mayo Clinic Rochester Institutional Review Board. HCC images were reviewed, and histological data were collected from The Cancer Genome Atlas (TCGA) data set by a liver pathologist (M.S.T.) using the https://portal.gdc.cancer.gov/ website. The TCGA collection consists of a single scanned slide for each case; for those cases with *CTNNB1*, *APC*, or *AXIN* mutations that originated from Mayo Clinic, the full set of slides from the original resection specimen was also reviewed to confirm the quality and representativeness of the TCGA image. Morphological findings were then correlated with clinical and sequencing data from TCGA, followed by gene expression analysis of specific subgroups, focusing on key morphological features such as pseudogland formation (Fig. 1).

2.2. Exclusions

After review, 41 TCGA cases were excluded for these reasons: no hematoxylin and eosin (H&E)-stained slide/poor quality H&E-stained slide/necrotic tumor/biopsy with insufficient material (n = 14); no sequencing information (n = 13); a diagnosis of HCC could not be confirmed on the scanned H&E (would need further evaluation to rule out hepatic adenoma or cholangiocarcinoma, n = 7); the H&E showed tumors that were not HCC (n = 5); and the same histological image was posted for different TCGA case numbers (n = 2).

2.3. Definition for beta-catenin-mutated morphology

In concordance with the literature, the classic morphology for beta-catenin-mutated HCCs was defined as the following: well-differentiated tumors with tumor cells having abundant eosinophilic cytoplasm, a thin trabeculae growth pattern (1—2 cells), and pseudoglands. Tumors with somewhat thicker trabeculae (5 cells or less in thickness), but otherwise classic morphology, were considered acceptable. To accommodate differences in H&E staining between cases, also acceptable were tumors with all of the preceding features but more amphophilic or basophilic cells. Cases were classified as having possibly compatible morphologies if (1) the tumor was well differentiated and had pseudoglands but had a predominately solid growth pattern; (2) the classic morphology was present, except for pseudoglands; or (3) the classic morphology was present except the tumor was not well differentiated.

2.4. Tumor grade

For grading tumors, the predominate grade was recorded, with the requirement that at least 5% of the tumor show the given grade when multiple grades were present. Tumor grades were assigned using the same criteria used in prior TCGA studies [1]. This approach is similar to that of the current WHO [8], with the addition of another grade for HCC with minimal cytological atypia: very-well-differentiated HCCs (grade 1) have no more than minimal cytological atypia; well-differentiated tumors (grade 2) show unequivocal hepatocellular differentiation on H&E, along with mild cytological atypia and/or mild architectural atypia; moderately differentiated tumors (grade 3) show

hepatocellular differentiation that is clearly present or strongly suspected from H&E, along with moderate cytological and or architectural atypia; poorly differentiated tumors (grade 4) showed marked cytological and or architectural atypia.

2.5. Tumor growth patterns

The predominate growth patterns in every tumor were classified as solid, pseudoglandular, trabecular, or macrotrabecular (trabeculae at least 10 cells in thickness).

2.6. Other histological findings

Macrovesicular steatosis was scored as positive or negative, with a minimal cut-off of 5%. Intratumoral lymphocytic inflammation was scored as none or minimal, mild, moderate, or marked (on average, more inflammatory cells than tumor cells). Bile within the tumor was scored as none, mild (less than 5% of tumor area), moderate (6—50% of tumor area), or marked (greater than 50% of tumor area). Intratumoral fibrosis was scored as none or minimal, mild (intratumoral fibrosis less than 5—25% of surface area), moderate (intratumoral fibrosis 26—50% of surface area), or marked (fibrosis is equal to or greater than the number of tumor cells). The percent surface area of the tumor involved by pseudoglands was scored as none, 1%, 5%, and then in 10% increments. The size of pseudoglands was scored as small (luminal diameter <2 tumor cell diameters), medium (luminal diameter 2—10 tumor cells in diameter), and large (luminal diameter 10 or more tumor cells in diameter). For analysis, cases were classified by the largest size of pseudoglands present in the section.

2.7. Statistical analysis

Categorical variables were compared using chi-square test, and numerical data were compared by Student's *t*-test or one-way analysis of variance, with *P* values <0.05 considered significant. Overall survival (OS) was defined as time from HCC diagnosis to death from any cause. The distribution of OS was estimated using the Kaplan—Meier methods and compared using the log-rank test and Cox proportional hazards model.

2.7.1. RNASeq gene expression analysis—The RNA sequencing (RNASeq) samples analyzed in this study were obtained by TCGA Research Network. TCGA-processed expression data were downloaded from Genomic Data Commons (GDC; https://gdc-hub.s3.us-east1.amazonaws.com/latest/TCGA-LIHC.htseq_counts.tsv.gz). Gencode's *Homo sapiens* hg38 assembly, v22, was used for the reference transcriptome, and GDC's GRCh38.d1.vd1 reference was used to define the human genome. The GDC RNASeq analysis pipeline leverages FASTQC and Picard Tools to assess the quality of the data and uses a combination of STAR and HTSeq to align the RNASeq reads and quantify gene expression. More details can be found at https://docs.gdc.cancer.gov/Data/Bioinformatics_Pipelines/Expression_mRNA_Pipeline/.

Genes with an average of ≥25 reads were kept for differential expression analysis. The R package, edgeR, was used to identify which genes were statistically differentially expressed from defined group comparisons. The categorical clinical metadata on these samples was used to define which samples belong to which groups. For each comparison, unsupervised

clustering was implemented with the ClustVis application on genes with a false discovery rate of <0.05 and with an absolute log2 fold change of >1.5 from the differential expression analysis. ClustVis was additionally used to visualize these findings through heat maps.

3. Results

A total of 338 cases had both histologic images of sufficient quality for review and molecular data, comprising seven fibrolamellar carcinomas and 331 conventional HCCs. A total of 128 tumors had mutations in *CTNNB1*, *APC*, or *AXIN* genes. There were 94 cases with *CTNNB1* mutations (one synonymous mutation and one intron mutation were classified as no mutation). Tumors showed *CTNNB1* mutations alone (N = 88), *CTNNB1* and *APC* mutations (N = 4), *CTNNB1* and *AXIN* mutations (N = 2), *AXIN* mutations alone (N = 26), *APC* mutations alone (N = 7), and *AXIN* and *APC* mutations (N = 1).

The predominant growth pattern in HCCs with *CTNNB1* mutations alone (without concomitant *APC* or *AXIN* mutations) were trabecular (N = 39/88, 44%), solid (N = 32/88, 36%), pseudoglandular (N = 12/88, 14%), and macrotrabecular (N = 5/88, 6%). In contrast, the remainder of the HCC were less likely to have pseudoglandular predominant growth patterns and more likely to have macrotrabecular predominant growth patterns ($P = 0.007$); growth patterns were as follows: trabecular (N = 126/250, 50%), solid (N = 91/250, 36%), pseudoglandular (N = 9/250, 4%), and macrotrabecular (N = 24/250, 10%).

CTNNB1 mutations were more common in men (80/231, 35%) than in women (14/107, 13%; $P = 0.000039$). In contrast, *APC* mutations did not differ in frequency between men (10/231, 4%) and women (2/107, 2%; $P = 0.26$). *AXIN* mutations also did not differ in frequency between men (19/231, 8%) and women (11/107, 10%; $P = 0.54$).

Cases with *APC* mutations, but lacking *CTNNB1* or *AXIN* mutations, were limited (N = 7), with two cases classified as having the classical *CTNNB1*-mutated morphology, three cases classified as possible *CTNNB1*-mutated morphologies, and two as showing non-*CTNNB1*-mutated morphologies. Given these results, tumors with *APC* mutations were included with *CTNNB1*-mutated tumors for subsequent analysis.

3.1. Classic CTNNB1-mutated HCC morphology

The classic morphological pattern associated with *CTNNB1*-mutated HCC was studied (Fig. 2; Table 1), with cases classified as having, possibly having, or not having the classic morphology. As expected, given the criteria used to identify the classic *CTNNB1* mutated morphological pattern, the classic pattern was strongly associated with the presence of pseudoglands ($P < 0.00001$) and bile production ($P < 0.00001$). The classic pattern was also associated with lower tumor grade: 42 of 63 (67%) of tumors with the classic morphology were very well or well differentiated, compared with 73 of 257 (28%) of tumors without the classic morphology. In addition, tumors with a classic *CTNNB1*-mutated morphology were less likely to have necrosis ($P = 0.004$).

The classic morphology was strongly associated with *CTNNB1* mutations ($P < 0.00001$), but not with *AXIN* mutations ($P = 0.5$). HCCs with *CTNNB1* mutations, however, were

histologically heterogeneous, with 58% (37/63) showing the classic morphology. *TP53* mutations were rare in tumors with the classic morphology (Table 1).

As tumors with possible and definite beta-catenin mutation morphologies appeared similar in most characteristics, they were combined for further analysis. There were at least five different *CTNNB1* specific missense mutations that were each present in at least five cases of HCC. Although the numbers are modest, the frequency of classic morphology varied sufficiently to suggest an association: S33P (4/5 have classic beta-catenin morphology), D32V (3/5), T41A (2/5), D32G (2/7), N387 (1/5), and K335I (0/5). Follow-up analysis of the affected codon, regardless of the specific mutation, further suggests that mutations in codons 335 and 387 are not associated with the development of the classic morphology (Supplemental Table 1).

3.2. Pseudogland formation and bile production

Pseudogland formation is an important component of the classic beta-catenin-mutated HCC morphological pattern, so the association with clinicopathological findings was further investigated as an independent variable (Table 2). As anticipated, there were strong associations with *CTNNB1*/*APC* mutations, lower tumor grade, bile production, and less frequent tumor necrosis. When analyzing the entire cohort of cases, male gender was strongly associated with the formation of pseudoglands ($P = 0.001$). Likewise, when analyzing the subset of HCCs with *CTNNB1*/*APC* mutations (N = 102), male gender was associated with the formation of pseudoglands ($P = 0.014$).

Once a tumor had pseudoglands present, neither the size of the pseudoglands nor the percent of the HCC with pseudoglands differed between men and women (Supplemental Table 2); moderate bile, however, was more common in HCC arising in men. In addition, once pseudoglands were present in a tumor, neither the percent of the tumor with pseudoglands nor the size of the pseudoglands correlated with the presence or absence of *CTNNB1*/*APC* mutations (Supplemental Table 3). Finally, the polyphen score for *CTNNB1* mutations did not correlate with classic morphology nor with the presence or absence of pseudoglands (Supplemental Table 4).

For tumors with pseudoglands and bile production, male gender was associated with moderate (versus mild) cholestasis (Supplemental Table 5). For carcinomas with pseudoglands in men, pseudoglands were associated with younger age (Supplemental Table 5). Younger aged men with tumors also showed more bile production (Supplemental Table 5). Together, these findings suggest that pseudogland formation and bile production are gender and age related, implying a role for androgen. Multivariate analysis to predicate pseudogland was then performed using age, gender, *CTNNB1* mutation, and *TP53* mutation. *CTNNB1* mutations were the most significant variable positively associated with pseudoglands (odds ratio [OR] = 3.2, $P = 2.5e\text{-}5$), followed by male gender (OR = 1.8), whereas *TP53* mutations predicated the absence of pseudoglands (OR = 0.5, $P = 0.01$). Age at diagnosis was not significant.

3.3. Gene expression analysis

To better understand if pseudogland formation is a homogenous process at the gene expression level, differential gene expression analysis was performed for the entire cohort of HCC, comparing all tumors with pseudoglands to all tumors without pseudoglands: 60 differentially expressed genes were identified. This set of 60 genes was then used to classify the entire cohort of all HCC and demonstrated three distinct clusters of tumors (Fig. 3A). Analysis of these three clusters showed that cluster 1 had a low frequency of pseudoglands, was enriched for younger age, female gender, and had a low frequency of *CTNNB1* mutations (Table 3). Cluster 2 was enriched for pseudoglands, male gender, and *CTNNB1* mutations. Cluster 3 was enriched for pseudoglands but had a low frequency of *CTNNB1* mutations. These same three clusters were then mapped to 21 known positive targets and two known negative targets of Wnt signaling (Supplement Table 6) [9] and identified a very strong correlation with cluster 2 (Fig. 3B). In addition, of the 23 genes in this panel, seven were statistically significant in their association with the formation of pseudoglands: *NKD1*, *NOTUM*, *REG3A*, *ODAM*, *RHBG*, *SLC1A2*, and *CYP2E1*. Together, these findings indicate that tumors with pseudoglands have a distinctive gene expression profile and that a subset of cases (cluster 2) is strongly associated with Wnt signaling. Unexpectedly, cluster 2 was also enriched for the cooccurrence of *CTNNB1* and *TP53* mutations (Table 2), and with clonal progression, defined as the same tumor showing multiple distinct morphologies [10]. This suggests that morphological features of *CTNNB1* mutations may be lost with tumor progression. Next, the analysis showed the set of 60 differentially expressed genes was significantly associated with the Wnt signaling pathway using GO Terms and Metascape, but not with IPA-canonical pathways (data not shown). Analysis of IPA upstream regulators, however, found *CTNNB1* to be the most important regulator.

Because of evidence that both *CTNNB1*/*APC* mutations and male gender are associated with pseudoglands, additional differential gene expression studies were performed controlling for these variables. First, the subset of tumors in women with *CTNNB1*/*APC* mutations was studied to see if gene expression could identify a signature associated with pseudogland formation. A set of 128 differentially expressed genes were identified and, when applied back to this same group, were able to completely separate tumors with pseudoglands (Fig. 4A). The same analysis in men identified 81 differentially expressed genes (Fig. 4B). Interestingly, there was little overlap in the differentially expressed genes associated with pseudoglands in tumors with *CTNNB1*/*APC* mutations for women versus men (Fig. 4C). These results indicate that pseudogland formation in HCC is associated with different gene expression pathways in men versus women, although both groups have *CTNNB1*/*APC* mutations.

3.4. Survival analysis

There was no difference in OS for patients who had HCCs with classic morphology, probable classic morphology, or nonclassic morphology (Fig. 4D); likewise, no survival differences were discernible for *CTNNB1* mutations versus no mutations (data not shown) or for pseudoglands versus no pseudoglands (Fig. 4E) in the overall cohort (5-year OS: 59.8% versus 58.6%). For HCCs with *CTNNB1* mutations, there appeared to be better survival in tumors that showed pseudoglands (5-year OS: 54.5% versus 37.4%), but the

results were not statistically significant, likely because of the small sample size, with survival data available for only 40 patients with HCC that had *CTNNB1* mutations (Fig. 4F).

3.5. HCC with CTNNB1 and or APC mutations and inflammation

Neither the classic morphology (Table 1) nor the presence of pseudoglands (Table 2) was associated with inflammation. A more detailed analysis of the subset of 102 cases with *CTNNB1*/*APC* mutations also found no clear association between the classic beta-catenin morphology and less inflammation (P = 0.2). Cases with classic morphology had no inflammation (N = 36), mild inflammation (N = 7), and moderate inflammation (N = 1); in contrast, HCC without the classic morphology had no inflammation (N = 39), mild inflammation (N = 15), and moderate inflammation (N = 4).

3.6. HCC with CTNNB1 and or APC mutations but without the classic morphology

A total of 58 cases had a *CTNNB1* or *APC* mutation but lacked the classic morphology and could be classified as having a not-otherwise-specified (NOS) morphology (N = 47) or could be classified into a recognized morphological subtype, including steatohepatitic (N = 5), scirrhous (N = 2), clear cell (N = 1), fibrolamellar carcinoma (N = 1), and lymphocyte rich (N = 1).

3.7. AXIN-mutated HCC

Twenty-six HCCs had *AXIN* mutations, without APC or *CTNNB1* mutations, including 17 men and nine women. This cohort had a younger average age of 54 ± 14 years, compared with patients whose HCCs had *CTNNB1* mutations alone ($P = 0.003$).

For the 26 cases with *AXIN* mutations, the predominate growth patterns were trabecular (n = 14), solid (n = 8), or macrotrabecular (n = 4). Seven cases (27%) had pseudoglands, and six cases (23%) had the classic morphology associated with beta-catenin mutations (four definite and two possible). The 20 cases without classic beta-catenin morphology showed these morphological patterns: NOS (n = 18), steatohepatitic (n = 1), and clear cell (n = 1).

4. Discussion

These findings affirm a strong association between *CTNNB1*-mutated HCCs and the morphological pattern of well-to-moderately differentiated tumors with thin trabeculae, pseudoglands, and bile production [3–5]. Tumors with the classic morphology were less likely to have *TP53* mutations, consistent with prior studies showing that *CTNNB1* and *TP53* mutations tend to be mutually exclusive, whether defined at the genetic [11] or protein expression levels [12]. Based on our findings, *APC* mutations in many cases lead to tumor morphology similar to that seen with CTTNB1 mutations, whereas *AXIN* mutations typically do not. Prior studies examining gene expression/function in human HCCs, cell culture experiments, and animal models have shown that *AXIN* mutations can promote HCC without activation of the Wnt signaling pathway [13,9], providing a potential explanation for our observation of the lack of a beta-catenin morphological signature in *AXIN*-mutated

tumors. In this study, *AXIN*-mutated HCCs presented at a younger age compared with *CTNNB1*-mutated tumors and generally had a NOS morphology.

In this study, *CTNNB1*-mutated HCCs were enriched for male gender. Likewise, within the subgroup of all HCCs with *CTNNB1*/*APC* mutations, the classic morphology was linked to male gender. A detailed analysis of morphology further showed that two key components of the classic beta-catenin-mutated HCC morphology are linked to male gender: pseudoglands and bile production. This association appears to be lost in older men, suggesting androgen may drive the development of pseudoglands and the production of bile. Prior studies provided potential mechanistic insights, showing that androgen receptor (AR) upregulates cell cycle—dependent kinase, driving tumorigenesis in a beta-catenin-dependent fashion [14]. Studies have also identified a positive feedback loop, wherein beta-catenin activation in turn upregulates AR. AR signaling can also lead to repression of Wnt pathway inhibitors via upregulation of EZH2 [15]. At the morphological level, these findings are further paralleled by observations in androgen-driven hepatic adenomas, which characteristically have pseudoglands and bile production [16]. These observations collectively indicate that male gender is not only associated with *CTNNB1* mutations, but that male gender in turn affects the gene penetrance of *CTNNB1* mutations in terms of distinct histological morphology. It remains unclear if *CTNNB1* mutations in the setting of higher levels of androgen expression also lead to differences in clinical behavior, such as prognosis or treatment response, but if so, future classifications may benefit by looking for a combined AR and Wnt signal within tumors. Given published results on the AR and Wnt pathway feedback loop [14], this group of patients may benefit from therapy that interrupts this feedback loop. This may have added clinical relevance, given that previous studies have suggested *CTNNB1* mutations promote resistance to anti-PD-1 therapy [7,6], which currently is a key component of the standard of care.

Specific genetic mutations are also relevant to the formation of pseudoglands, presumably engendering stronger Wnt signaling. In this study, neither K335 nor N387 *CTNNB1* mutations were consistently associated with the classic beta-catenin-mutated morphology. In keeping with these results, prior studies have shown that these two mutations only weakly activate the Wnt signaling pathway in cell culture [17]. Together, these findings suggest that future molecular-based classification systems will be improved as they incorporate the specific *CTNNB1* mutation.

In this study, 58% of HCCs with *CTNNB1* mutations had the classic morphology. One of the limitations of this study is that most cases had a single scanned slide for histological review, and HCC can be morphologically heterogenous. Nonetheless, the results in this study are very similar to the results of prior studies [3–5], indicating that 40% of *CTNNB1*-mutated HCCs do not have the classic morphology. In this study, those cases without the classic morphology could be classified into a specific subtype (10%), such as steatohepatitic or scirrhous HCC, or had a NOS morphology (30%).

Differential gene expression analysis examined the gene expression profile of tumors with and without pseudoglands and identified two distinct clusters of HCC with pseudoglands: clusters 2 and 3. Interestingly, only cluster 2 was associated with the expression of

downstream targets of the Wnt signaling pathway and with *CTNNB1* mutations, suggesting other signaling pathways can also drive pseudogland formation, as shown by cluster 3. Also of note, although cluster 2 was strongly linked to Wnt pathway activation, only 50% of the tumors had the classic morphology associated with beta-catenin mutations. These latter results suggest that morphology is insufficient to reliably identify subsets of HCC with either beta-catenin mutations or with gene expression indicative of Wnt signaling activation. Part of the explanation for the discrepancy between mutation status and morphology may be that in some cases, the *CTNNB1* mutations are late events and not true drivers of the tumor growth. An additional possibility is suggested by further analysis of cluster 2, which showed this cluster was enriched for the presence of shared *CTNNB1* and *TP53* mutations and was more likely to show clonal progression; these areas of clonal progression may show a different and less well-differentiated morphology. *CTNNB1*/*APC* mutations in men versus women also led to distinct gene expression patterns with relatively little overlap. The explanation for this is unclear, but possibilities include the effects of androgens as well the possibility of different timing of mutations in the process of carcinogenesis.

The results from this study identify key factors that influence heterogeneity in the morphology of *CTNNB1*-mutated tumors: (1) specific *CTNNB1* mutation and (2) gender, but other possibilities include (3) tumor dedifferentiation as well as (4) tumors where *CTNNB1* is potentially not the main driver mutation, possibly representing passenger or late-driver mutations [18]. This heterogeneity represents a challenge for sequencing-based classification schemas. Our findings indicate that those HCC with *CTNNB1* mutations that occur in men are most likely to be associated with the classic morphology and to be enriched for differentially expressed genes within the Wnt signaling pathway; it is this group (cluster 2) that appears to form the most cohesive morphomolecular group. The observation that some cases have the classic morphology associated with *CTNNB1* mutations and/or pseudoglands, but lack *CTNNB1* mutations, suggests there are additional pathways that converge on these morphological patterns.

In conclusion, *CTNNB1*-mutated HCCs are histologically heterogeneous. Factors that influence the morphological findings include gender and the specific mutation site in the gene. These morphological observations can be used to improve the morphomolecular classification of *CTNNB1*-mutated HCCs.

Supplementary Material

Refer to Web version on PubMed Central for supplementary material.

Acknowledgments

Grant support: P50 CA210964 (M.S.T., J.Y., R.R.L., and C.W.).

Abbreviations:

HCC	hepatocellular carcinoma

References

[1]. Cancer Genome Atlas Research Network. Electronic address wbe, Cancer Genome Atlas Research N. Comprehensive and integrative genomic characterization of hepatocellular carcinoma. Cell 2017; 169:1327e41. e23.

[2]. Nhieu JT, Renard CA, Wei Y, Cherqui D, et al. Nuclear accumulation of mutated beta-catenin in hepatocellular carcinoma is associated with increased cell proliferation. Am J Pathol 1999;155:703–10. [PubMed: 10487827]

[3]. Audard V, Grimber G, Elie C, Radenen B, et al. Cholestasis is a marker for hepatocellular carcinomas displaying beta-catenin mutations. J Pathol 2007;212:345–52. [PubMed: 17487939]

[4]. Dal Bello B, Rosa L, Campanini N, Tinelli C, et al. Glutamine synthetase immunostaining correlates with pathologic features of hepatocellular carcinoma and better survival after radiofrequency thermal ablation. Clin Canc Res 2010;16:2157–66.

[5]. Kitao A, Matsui O, Yoneda N, Kozaka K, et al. Hepatocellular carcinoma with beta-catenin mutation: imaging and pathologic characteristics. Radiology 2015;275:708–17. [PubMed: 25668519]

[6]. Ruiz de Galarreta M, Bresnahan E, Molina-Sanchez P, Lindblad KE, et al. Beta-catenin activation promotes immune escape and resistance to anti-PD-1 therapy in hepatocellular carcinoma. Canc Discov 2019; 9:1124–41.

[7]. Harding JJ, Nandakumar S, Armenia J, Khalil DN, et al. Prospective genotyping of hepatocellular carcinoma: clinical implications of next-generation sequencing for matching patients to targeted and immune therapies. Clin Canc Res 2019;25:2116–26.

[8]. Digestive systems tumors. 5th ed. Lyon, France: International Agency fo Research on Cancer; 2019.

[9]. Abitbol S, Dahmani R, Coulouarn C, Ragazzon B, et al. AXIN deficiency in human and mouse hepatocytes induces hepatocellular carcinoma in the absence of beta-catenin activation. J Hepatol 2018; 68:1203–13. [PubMed: 29525529]

[10]. Torbenson MS. Hepatocellular carcinoma: making sense of morphological heterogeneity, growth patterns, and subtypes. Hum Pathol 2020.

[11]. Laurent-Puig P, Legoix P, Bluteau O, Belghiti J, et al. Genetic alterations associated with hepatocellular carcinomas define distinct pathways of hepatocarcinogenesis. Gastroenterology 2001;120: 1763–73. [PubMed: 11375957]

[12]. Torbenson M, Kannangai R, Abraham S, Sahin F, et al. Concurrent evaluation of p53, beta-catenin, and alpha-fetoprotein expression in human hepatocellular carcinoma. Am J Clin Pathol 2004;122: 377–82. [PubMed: 15362367]

[13]. Zucman-Rossi J, Benhamouche S, Godard C, Boyault S, et al. Differential effects of inactivated AXIN1 and activated beta-catenin mutations in human hepatocellular carcinomas. Oncogene 2007;26: 774–80. [PubMed: 16964294]

[14]. Feng H, Cheng AS, Tsang DP, Li MS, et al. Cell cycle-related kinase is a direct androgen receptor-regulated gene that drives betacatenin/T cell factor-dependent hepatocarcinogenesis. J Clin Invest 2011;121:3159–75. [PubMed: 21747169]

[15]. Song H, Yu Z, Sun X, Feng J, et al. Androgen receptor drives hepatocellular carcinogenesis by activating enhancer of zeste homolog 2-mediated Wnt/beta-catenin signaling. EBioMedicine 2018;35: 155–66. [PubMed: 30150059]

[16]. Gupta S, Naini BV, Munoz R, Graham RP, et al. Hepatocellular neoplasms arising in association with androgen use. Am J Surg Pathol 2016;40:454–61. [PubMed: 26685086]

[17]. Rebouissou S, Franconi A, Calderaro J, Letouze E, et al. Genotype-phenotype correlation of CTNNB1 mutations reveals different sscatenin activity associated with liver tumor progression. Hepatology 2016;64:2047–61. [PubMed: 27177928]

[18]. Friemel J, Rechsteiner M, Frick L, Bohm F, et al. Intratumor heterogeneity in hepatocellular carcinoma. Clin Canc Res 2015;21:1951–61.

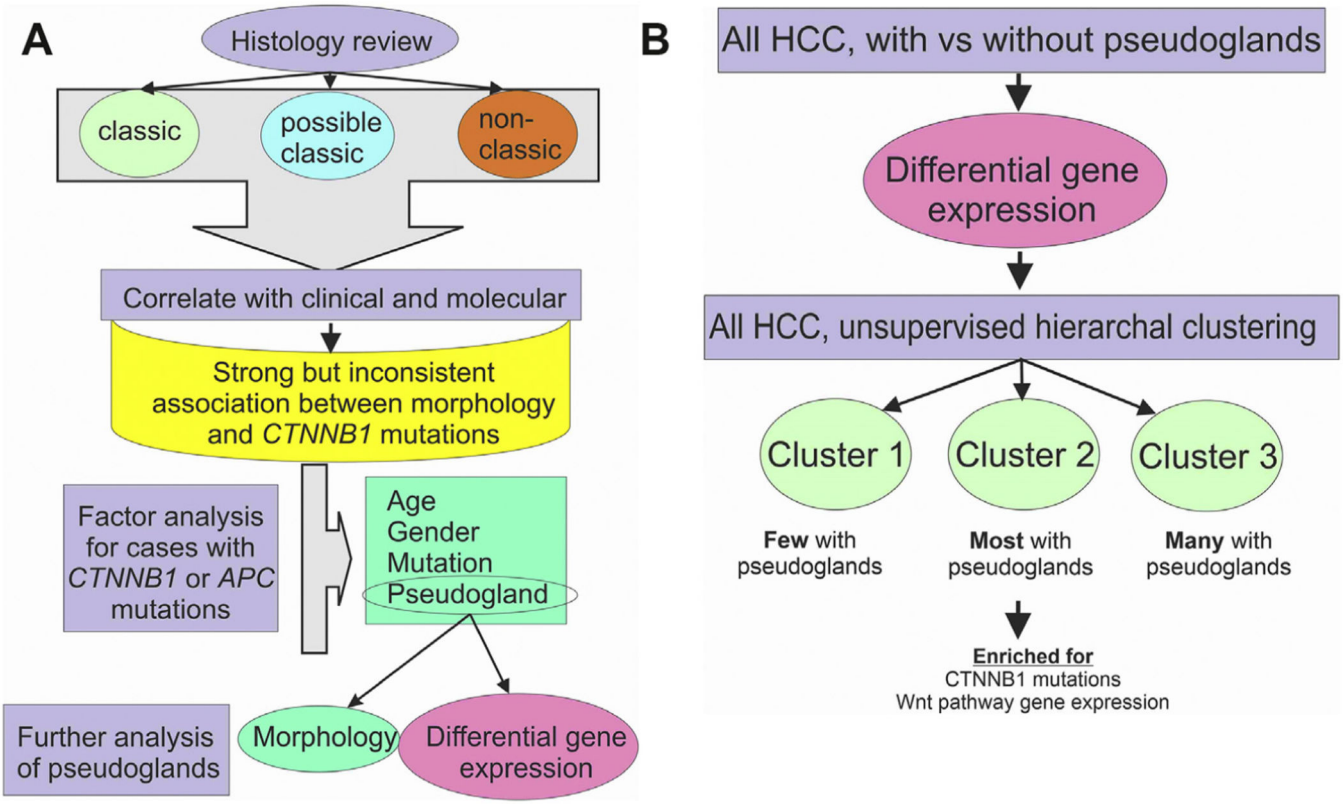

Fig. 1. Study design.

(Panel A) The histology was reviewed and classified without regard to clinical or sequencing results. Next, the histology was correlated with clinical and sequencing results, identifying a strong but inconsistent relationship. Factor analysis then focused on cases with CTNNB1 or APC mutations to identify correlates of the classic morphology. This was followed up by subset analysis of cases with pseudoglands. (Panel 2B) Approach for analysis of cases with pseudoglands. In the first step, HCCs were divided by morphology into those with and without pseudoglands. DGE identified a specific set of gene expression associated with pseudoglands. This set of DGE was then used to classify HCC without regards to morphology or mutation status and identified three distinct clusters.

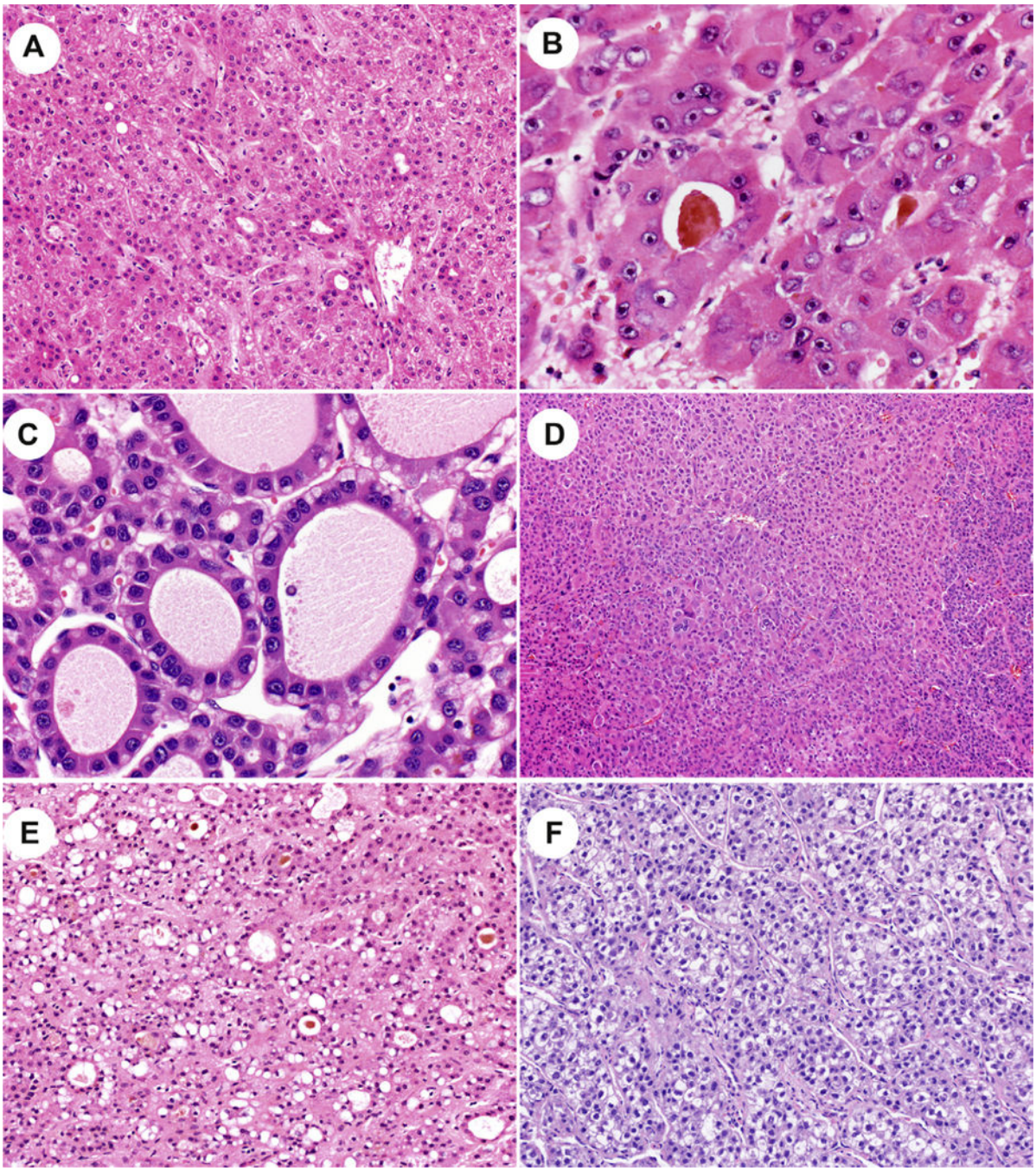

Fig. 2. Morphological findings.

(Panel A) The classic beta-catenin morphology with thin trabeculae and pseudoglands. (Panel B) A higher power image of pseudoglands. (Panel 1C) Bile production is seen. (Panel 1D) This beta-catenin-mutated hepatocellular carcinoma lacks the classic morphology. (Panel 1E) This *APC*-mutated hepatocellular carcinoma shows the classic morphology. (Panel 1F) This AXIN-mutated hepatocellular carcinoma lacks the classic morphology.

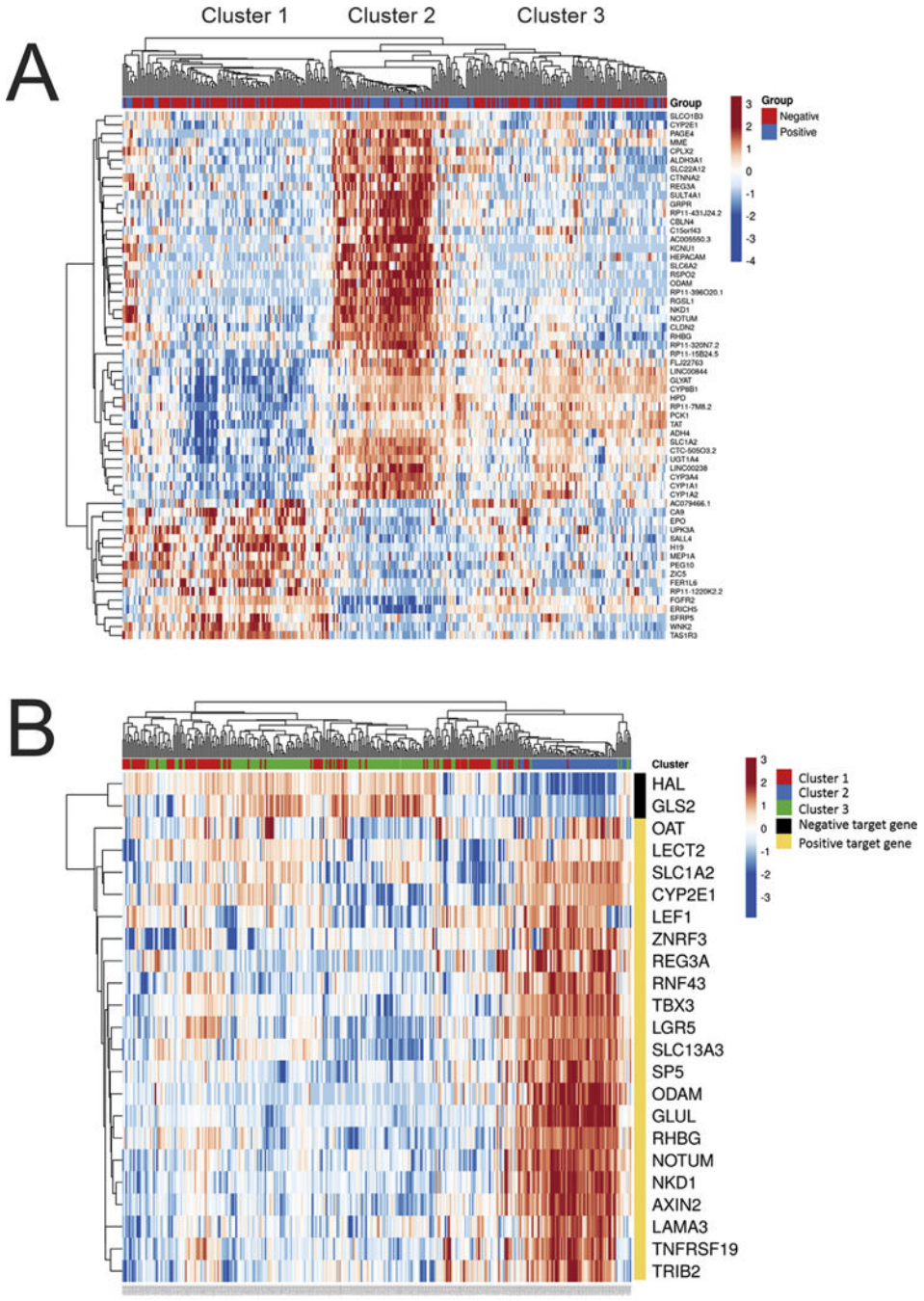

Fig. 3. Pseudoglands, differential gene expression analysis.

The differentially expressed (DE) genes in HCC with pseudoglands versus without pseudoglands was studied in the entire set of study cases, as well several subsets, which controlled for factors that likely influence pseudogland formation, namely, gender and *CTNNB1* mutations. The DE genes identified in each study were then used to classify HCC within the cohort to see if the selected genes accurately predicted pseudogland formation, and the results are shown as heat maps. In the top bar, blue indicates pseudoglands were present, and red indicates their absence. (**Panel A**) A total of 60 DE genes were identified

when examining all cases with sufficient histology and gene expression data (N = 333). When the 60 DE genes were used to classify the HCC, three distinct groups/clusters emerged. (**Panel B**) These three clusters were then mapped to expression of genes known to be regulated by *CTNNB1*. Cluster 2, but not clusters 1 and 3, is strongly associated with genes regulated by *CTNNB1*. (For interpretation of the references to colour in this figure legend, the reader is referred to the Web version of this article.)

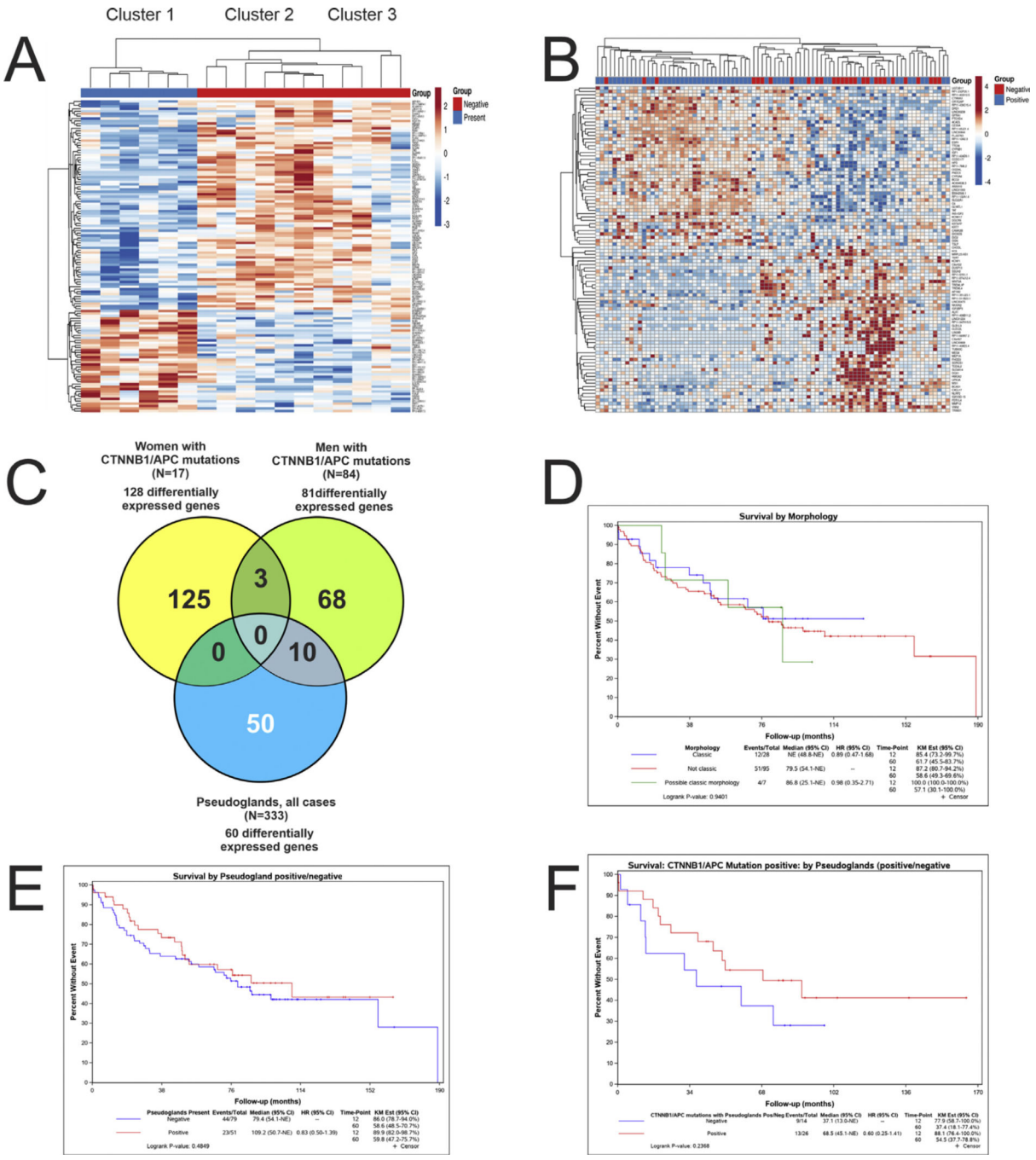

Fig. 4. Pseudoglands, gender, survival.

(Panel A) DE gene expression for HCC in women with *CTNNB1* mutations identified 128 DE genes. This set of 128 DE genes could accurately classify all cases in this cohort as having or not having pseudoglands. (**Panel B**) DE gene expression for HCC in men with *CTNNB1* mutations identified 81 DE genes. This set of 81 DE genes could classify cases as having or not having pseudoglands with moderate accuracy. (**Panel C**) DE genes that predicated pseudogland formation showed relatively little overlap between the three groups. (**Panel D**) No survival differences are seen in patients whose HCC have the

classic, possible classic, or nonclassic morphology for *CTNNB1* mutations. (**Panel E**) No survival differences are seen in patients whose HCC have pseudoglands versus HCC without pseudoglands. (**Panel F**) Patients with HCC that had *CTNNB1* mutations and pseudogland formation had better survival, but the results are not statistically significant.

Table 1

Clinical, morphological, and mutational correlates of hepatocellular carcinoma with the classic beta-catenin mutation morphology of thin trabeculae, pseudoglands, and often bile.

	Classic morphology	**Possible classic morphology**	**Not classic morph**	***P***
Total	63	18	257	
Age	60 ± 14	59 ± 12	58 ± 14	0.6
Gender				0.17
Male	49	13	169	
Female	14	5	88	
Ethnicity				0.462 (grouped together: Hispanic, native American and not stated)
White	25	5	122	
Asian	32	12	112	
Black	4	0	9	
Hispanic	1	1	8	
Native American	0	0	1	
Not stated	1	0	5	
Tumor subtype				
NOS	61	17	190	
Steatohepatitic	0	1	21	
Scirrhous	0	0	18	
Clear cell	2	0	12	
FLC	0	0	7	
Lymphocyte rich	0	0	3	
Cirrhotomimmetic	0	0	3	
Sarcomatoid	0	0	2	
Myxoid	0	0	1	
Tumor grade (predominate)				<0.001
1	8	3	18	
2	33	3	55	
3	19	8	120	
4	3	4	64	

	Classic morphology	Possible classic morphology	Not classic morph	*P*
NA				
Tumor necrosis				0.004
Yes	5	1	63	
No	58	17	194	
Tumor hyaline bodies				0.46
Yes	9	2	50	
No	54	16	207	
Pseudoglands				<0.001
Yes	63	11	58	
No	0	7	199	
Tumor bile				<0.001
Yes	33	4	42	
No	30	14	215	
Tumor inflammation				0.80
Yes	15	5	72	
None or minimal	48	13	185	
Tumor steatosis (>5%)				0.09
Yes	10	2	68	
No	53	16	189	
Tumor fibrosis				0.004
Yes	7	3	79	
No	56	15	178	
No. somatic mutations	161 + 100	164 + 71	170 + 199	0.6
Any Wnt mutation (CTNNB1, AXIN, APC)				<0.001
Yes	41	9	78	
No	22	9	179	
CTNNB1 mutation alone				<0.001
Yes	34	3	51	
No	29	15	206	
AXIN mutation alone				0.54

Hum Pathol. Author manuscript; available in PMC 2023 January 01.

	Classic morphology	Possible classic morphology	Not classic morph	*P*
Yes	4	2	20	
No	59	16	237	
CTNNB1 and/or APC				<0.001
Yes	37	7	58	
No	26	11	199	
TP53 mutation alone (point, indel, or CNV-loss)				<0.001
Yes	10	4	157	
No	53	14	100	
CTNNB1 and TP53 mutation				0.88
Yes	4	1	20	
No	59	17	237	

*Excluding clonal progression.

Table 2

Clinical, morphological, and mutational correlates of pseudoglands.

Factor	Total	Pseudoglands present	Pseudoglands negative	*P* (yes versus no pseudoglands)
Total	338	132 (39%)	206 (61%)	
Gender				0.001
Male	231	104 (45% of gender)	127 (55%)	
Female	107	28 (26%)	79 (74%)	
Age (mean ± SD)				
All	58.5 ± 13.8	59.5 ± 14.2	58.0 ± 13.4	0.31
Male	57.8 ± 12.9	59.4 ± 12.6	56.5 ± 13	0.10
Female	60.2 ± 15.3	60.0 ± 18.9	60.2 ± 14.0	0.96
Ethnicity				0.32 (grouped together: Hispanic, native American and not stated)
White	159	61	91	
Asian	157	56	100	
Black	14	8	5	
Hispanic	10	5	5	
Native American	1	0	1	
Not stated	6	2	4	
Tumor subtype				0.002392 (FLC and below grouped together)
NOS	275	116	152	
Steatohepatitic	22	3	19	
Scirrhous	21	2	16	
Clear cell	14	3	11	
FLC	6	5	2	
Lymphocyte rich	3	1	2	
Cirrhotomimmetic	3	2	1	
Sarcomatoid	2	0	2	
Myxoid	1	0	1	
Tumor grade predominate				0.014
1	22	10	19	
2	71	48	43	

Factor	Total	Pseudoglands present	Pseudoglands negative	*P* (yes versus no pseudoglands)
3	148	53	94	
4	103	21	50	
Tumor necrosis				0.002
Yes	69 (20%)	16 (12%)	53 (26%)	
No	269 (80%)	116 (78%)	153 (74%)	
Tumor hyaline bodies				0.155
Yes	43 (44%)	15	35	
No	304	117	171	
Tumor bile				<0.0001
Yes	79	64	15	
No	288	68	191	
Tumor inflammation				0.33
Yes	93	32	60	
No	254	100	146	
Tumor steatosis (>5%)				0.057
Yes	80 (24%)	24	56 (x%)	
No	258	108	150	
Tumor fibrosis				0.5
Yes	95	27	62	
No	252	105	144	
No. somatic mutations				
All	166 ± 177	170 ± 172	167 ± 184	0.89
Male	179 ± 203	181 ± 189	177 ± 218	0.90
Female	141 ± 100	128 ± 69	150 ± 111	0.33
Any Wnt mutation (CTNNB1, AXIN, and APC)				<0.001
Yes	128	70	58	
No	210	62	148	
CTNNB1 mutation				<0.001
CTNNB1 mutation alone	88	55	33	
CTNNB1 + AXIN/APC	6	3	3	
No CTNNB1 mutation	244	74	170	

Hum Pathol. Author manuscript; available in PMC 2023 January 01.

Factor	Total	Pseudoglands present	Pseudoglands negative	*P* (yes versus no pseudoglands)
AXIN mutation				0.34
AXIN mutation alone	26	7	19	
AXIN + CTNNB1/APC	3	0	3	
No AXIN mutation	309	125	184	
CTNNB1 and or APC				<0.001
Yes	104	63	39	
No	243	69	167	

Hum Pathol. Author manuscript; available in PMC 2023 January 01.

Table 3

Three case clusters identified by differential gene expression analysis.

	Cluster 1	Cluster 2	Cluster 3	P
N	110	66	142	
Gender M/F (ratio)	58/52	56/10	104/38	0.00001
Age (average ± SD)	55.5 ± 12	61.6 ± 13	60 ± 14	0.005
Pseudoglands	22 (20%)	43 (65%)	57 (40%)	<0.00001
CTNNB1/APC mutations	14 (13%)	58 (88%)	25 (18%)	<0.00001
AXIN mutations	20 (18%)	0	7 (5%)	<0.00001
Classic beta-catenin morphology	15 (14%)	33 (50%)	28 (20%)	<0.00001
CTNNB1 mutations and classic beta-catenin morphology	2 (2%)	28 (42%)	10 (7%)	<0.00001
Intratumoral inflammation	37 (33%)	15 (23%)	37 (45%)	0.23
Ploidy (average ± SD)	2.9 ± 1	2.5 ± 0.8	2.4 ± 0.7	0.00013
TP53 mutations	44 (40%)	18 (26%)	44 (31%)	0.22
Combined *CTNNB1* and *TP53* mutations	6 (5%)	17 (26%)	2 (1%)	
	0 with clonal progression	8 with clonal progression		
HBV infection	25 (23%)	21 (32%)	27 (19%)	0.12